International Journal of Electrical and Computer Engineering (IJECE)
Vol. 14, No. 2, April 2024, pp. 1382~1389
ISSN: 2088-8708, DOI: 10.11591/ijece.v14i2.pp1382-1389 ❒ 1382

Plasmonic wave assessment via optomechatronics system for biosensor application

Muhammad Rosli Abdullah[1], Noor Hasmiza Harun[1], Siti Noorjannah Ibrahim[2], Azimah Abdul Wahab[3], Mohd Azerulazree Jamilan[4]
[1]Medical Engineering Technology Section, University of Kuala Lumpur-British Malaysian Institute, Selangor, Malaysia
[2]Department of Electrical and Computer, Engineering International Islamic University, Selangor, Malaysia
[3]Medical Science Technology, Universiti Kuala Lumpur-Institute of Medical Science Technology, Selangor, Malaysia
[4]Nutrition, Metabolism, and Cardiovascular Research Centre, Institute for Medical Research, Ministry of Health Malaysia, Selangor, Malaysia

Article Info

Article history:

Received Jul 13, 2023
Revised Sep 25, 2023
Accepted Nov 12, 2023

Keywords:

Biosensor
Electromagnetic
Microstepping
Optomechatronics
Plasmonic
P-polarized
Resonance

ABSTRAC

Transduction biosensor (mass-based, optical and electrochemical) involves analysis, recognition and amplification in the acquired sample. In this work, the plasmonic-based biosensor was employed without using tags. It is crucial to determine angles of Brewster (ϴb) and critical (ϴc) for generating plasmonic resonance (ϴr). The objective is to verify a cost-effective plasmonic biosensor through Fresnel simulation and experimentation of a developed optomechatronics system. The borosilicate glass, Au and Air layers were simulated with the Winspall 3.02 simulator. The optomechatronics system consists of: 1-optics (650 nm laser, slit, polarizer, photodiode), 2-mechanical (bipolar stepper motors, gears, stages) and 3-electronics (PIC18F4550, liquid crystal display (LCD) and drivers). Later, the software performs angular interrogation by reading the reflected beam from a rotating prism at 0.1125. Experimentation to simulation accuracy indicates that percentage differences for ϴr and ϴc are 1% and 0.2%, respectively. In conclusion, excellence verification was successfully achieved between experimentation and simulation. It proved that the low-cost optomechatronics system is capable and reliable to be deployed for the biosensor application.

Corresponding Author:

Muhammad Rosli Abdullah
Department of Medical Engineering Technology Section, Faculty of Engineering, University of Kuala Lumpur–British Malaysian Institute
Batu 8, Sungai Pusu street, 53100, Selangor, Malaysia
Email: rosli@unikl.edu.my

1. INTRODUCTION

Biosensors quantify biological signals via bio-recognition, bio-transducer, and electronics systems [1]. Many biosensors require labeling substances such as fluorescent, isotopic, chemiluminescent, radioactive, quantum dot, antibodies, nanoparticles, and enzymes [2]. Purchasing test kits and labeling molecules for a biosensor will incur extra costs [3], [4]. Conversely, plasmonic-based biosensors promote a label-free method for instant measurement, cheaper procedures, low sample volume, high sensitivity and specificity [5], [6]. Unfortunately, more is required to know about the production of the plasmonic wave for a label-free biosensor. It becomes relevant to assess a beam reflectivity for verifying the plasmonic wave under reference to angles of Brewster, critical and resonance. Demand for reliable, low-cost biosensors is rising globally due to rising healthcare costs [7]. However, a low-cost biosensor without compromising system accuracy is highly desirable.

Therefore, a strategy for cost-effectiveness plasmonic-based biosensors should be reported via 3D printing for the optomechatronics system. Label-free biosensors are tested for optical, dielectric permittivity, acoustic, electrochemical, and electrical impedance [8]–[11]. During the coronavirus disease (COVID-19) pandemic, research in optical biosensors was expedited for coronavirus [6]. The modulation/transduction methods assessed/evaluated optical properties (transmission, absorption, reflection, refraction, scattering, and plasmonic) [12]. Later, these properties are applied in optical biosensor applications such as plasmonic, spectroscopy, colorimetric, interferometric, luminescent, fluorescent and evanescent waves [13]. Optical biosensors monitor affinity, binding kinetics, concentration, and specificity [14]. Bio-receptors for the optical biosensor include antibodies, aptamers, enzymes, nuclear acids, and molecularly imprinted polymers [15]–[19].

Bioreceptors replicate physiological interactions to bind chemicals on sensor surfaces [19]. Optical-bioreceptor have benefits in biotechnology, nanotechnology, molecular biology, microbiology, virology, and chemistry [20]. Optical, mechanical, and electronics collaboration allows spectral investigation on dielectric-metal interfaces [21], [22]. The collaboration synchronizes opto-mechanical positions for high-accuracy and repeatability measurements. Photons at total internal reflection (TIR) excite a positive-negative permittivity of the dielectric-metal interfaces to create plasmonic energy [23]. Photon intensity is significantly reduced by plasmonic energy absorption [24]. This phenomenon is known as a resonance angle caused by the penetration of plasmonic energy from lower to upper interfaces of dielectric-metal [25]. It is proportional to the refractive index of any biological substance deposited on the metal interface. An optical biosensor with computational validation for *Escherichia coli* (E.coli) was carried out. It consists of functionalized (polyclonal anti-E.coli antibody) polymer optical fiber (POF), light emitting diode (LED), photodetector and data acquisition (DAQ) card. Detection of E-coli is successfully obtained with a concentration of 104 CFU/ml. However, a characteristic of hydrophilic or hydrophobic contact on the antigenic regions must be pre-identified for epitope prediction with computer validation [26].

In a similar work, a selective and sensitive biosensor had been designed with the photonic crystal for ethanol and methanol detection. A different concentration of ethanol/ methanol percentages correlated with a change in the refractive indexes (r.i). Ethanol/methanol with water mixtures shows different detection spectra at 1.2/1.4 nm with 1.3326/1.36212 r.i from 1,369 to 1,391.5 nm of resonance wavelength [27]. High sensitivity, quality factor, figure of merit and transfer coefficient were achieved respectively at 750 nm/RIU, 1000, 561 RIU−1 and 97%. However, no linearity between densities and refractive index was recorded for different alcohol percentages.

Despite the availability of numerous biosensors in the market, the optomechatronics system presents a viable alternative to existing commercial solutions. The objectives are to i) develop a cost-effective plasmonic-based biosensor and ii) assess/validate the existence of the plasmonic wave via Fresnel simulation/ optomechatronics system, respectively.

2. RESEARCH METHOD

This section discusses the simulation and development of optomechatronics for optics, mechanical systems, and electronic systems. The optics involve a p-polarized beam for Transverse Magnetic transmission. The p-polarized beam then hits the prism and reflects to a photodiode in a single rotation. Therefore, the prism-photodiode was positioned and aligned mechanically on rotational stages. The photodiode converts the received beam into voltages and feeds to the electronics section. The section performs: i) photodiode digitization, ii) stepper motor synchronization, and iii) serial transmission of reflective data to the computer.

2.1. Simulation

Winspall is a software to simulate reflectivity curves as expressed by the Fresnel equation in (1) and (2). The equations determine electromagnetic wave transmission and reflection at different refractive index mediums (n_1 and n_2) and permeability (μ_1 and μ_2).

$$r_p = \frac{(n_1/\mu_1)\cos\theta_t - (n_2/\mu_2)\cos\theta_i}{(n_1/\mu_1)\cos\theta_t + (n_2/\mu_2)\cos\theta_i} \quad (1)$$

$$t_p = \frac{2(n_2/\mu_2)\cos\theta_i}{(n_1/\mu_1)\cos\theta_t + (n_2/\mu_2)\cos\theta_i} \quad (2)$$

The simulation parameter offers permittivity $(e' + ie'')$ or refractive index $(n + ik)$, respectively for inputting layers thickness/ dielectric constant or layer thickness/ refractive index. As shown in Table 1, different dielectric layers are used to simulate plasmonic resonance.

Table 1. Dielectric constant

layers	Medium	Thickness (nm)	EpsX-real	EpsX-imaginary
1	BK7 glass	0	2.29	0
2	Gold (Au)	50	-12.45	1.3
3	Air	0	1	0

2.2. Optomechatronics system

The system in Figure 1 consists of several operating interfaces such as optics, electronics, mechanical and PC-based control systems. Thorlabs laser diode (650 nm, 7 mW) was chosen as a monochromatic light source. Two aspheric lenses (f =20.1 mm) converged the light source to the thin gold (Au) film at 50 nm. Adjustable aperture control via the iris was aligned and positioned accurately to reduce the diffraction effect. A linear polarizer is vital to assure TM or P-polarized excitation under a Brewster angle, as expressed in (3) [4].

$$\theta_{B=}\tan^{-1}(n_2/n_1) \tag{3}$$

Two prisms (coated Au layer at 50 nm and non-coated) were tested for acquiring p-polarized light and generating plasmonic resonance. They were placed on a rotating optical stage to achieve a reflectivity profile via a photodiode from 30° to 80° of the incidence angles.

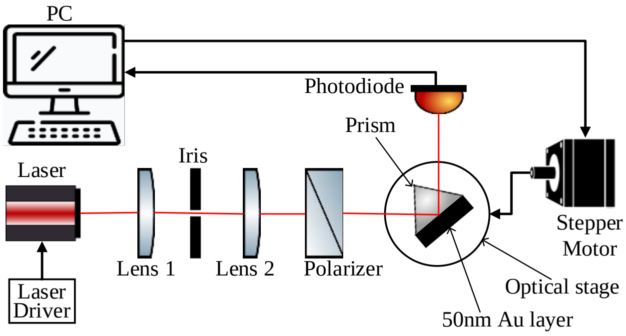

Figure 1. Optics schematic diagram

The mechanical design in the Figure 2 is based on replaceable modular parts such as gears, stages, stands, plates, cages, bases, couplers, holders and sockets. The annular gear (AG) functions as the photodiode (PD) stage and is coupled to the running gear (RG). The RG was fitted to the stepper motor and housed with dual support gears (SG). Due to the expensive optic components in the market, 3D models are respectively shown on Side/ Top views in Figure 2(a) and Figure 2(b) were designed and sliced.

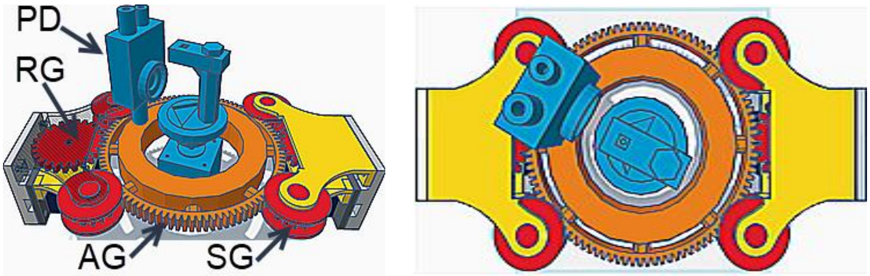

(a) (b)

Figure 2. Design of optomechatronics system: (a) side view and (b) top view

The electronic system in Figure 3 converts acquired reflectance from the photodiode (PD) at a 1.6 µs interval via an onboard 10-bit analog digital converter (ADC)'s PIC18F4550. The ADC reference voltage was set to 2 V for 1.95 mV ADC resolution to satisfy PD's voltage range. The ADC results were sampled and averaged 150 times to eliminate fluctuation due to the 50 Hz power line interference. Then, ADC's result was sent to the personal computer (PC) at 19,200 bps via asynchronous serial. Apart from ADC reception, the PC interface also: 1- Choose 18 modes of the stepper motor, 2- control and synchronize the stepper motor (SM1 and SM2), 3- Data logging and 4- Digital filtering for smoothing ADC data with Savitzky Golay as expressed in (4).

$$y_t = \frac{(-2x_{t-3}+3x_{t-2}+6x_{t-1}+7x_t+6x_{t+1}+3x_{t+2}-2x_{t+3})}{21} \quad (4)$$

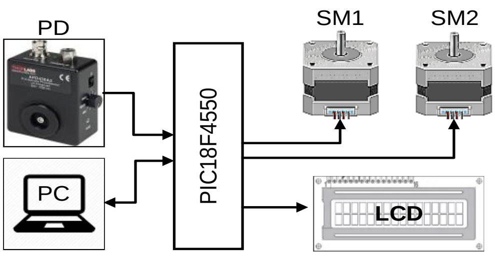

Figure 3. Electronic system for optomechatronics system

3. RESULTS AND DISCUSSION

As shown in Figure 4, the mechanical system had been fabricated and assembled. The photodiode (PD) stage was retrofitted to the annular gear (AG), and the prism was placed on the rotational stage (RS). The gear teeth at a 2.5 ratio for AG and running gear (RG) are set to 145 and 58, respectively.

Different trains of pulses (Top trace) were generated in Figure 5 for AG at every T-pulse (Bottom trace) of the rotational stage (RS). The generated number of AG's pulses (ps) was changed from 2ps to 3ps at T intervals to fulfill the 2.5 gear ratio. It synchronizes PD/ RS at 0.1125°/0.045° resolution for 3,200/8,000 steps on a single rotation, respectively.

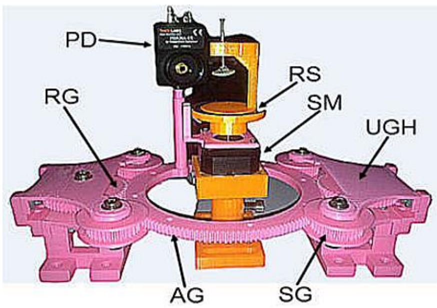

Figure 4. Fabricated and assembled of an optomechatronics system with a 3D printer

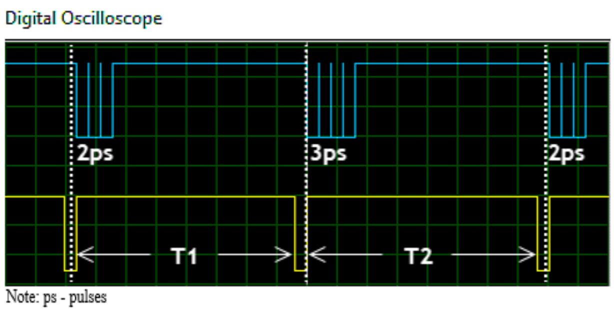

Figure 5. Stepper motor pulses for the photodiode stage and prism stage

The P-polarized wave was confirmed with a non-coated prism, as observed as a reflectivity trace (dash line) in Figure 6. When the incidence angle (θi) gradually increases, the reflectivity decreases until it hits zero intensity at Brewster angle (θB). Beyond θB, the θi keeps rising until the transmitted angle (θt) is equal to 90°. At this point, reflectivity becomes saturated for the total internal reflection (TIR) condition at $\theta i>\theta_{C2}$. Therefore, a linear polarizer (400~700 nm) was rotated via rotation mount (RSP1/M) for generating P-polarized light at Brewster's angle. Meanwhile, a solid line in Figure 6 represents a reflective trace from a 50 nm gold (Au) layer coated on the prism. A maximum attenuation was observed at the resonance angle (θres) due to the excitation of plasmonic energy beyond the critical angle (θ_{C1}). However, the plasmonic energy could not be generated from the non-coated prism as observed from a flat reflectivity trace beyond the critical angle (θ_{C2}). Resonance occurs when energy conservation (angular frequency of incident light) matches the momentum (k-propagation) for generating the plasmonic energy.

In Figure 7, the experimentation result indicates reflectivity curves from the photodiode at different reflected angles and stepper motor steps. Measured reflectivity traces via the developed optomechatronics system were plotted in Figure 7(a) and Figure 7(b) for the non-coated and Au-coated prism (50 nm), respectively.

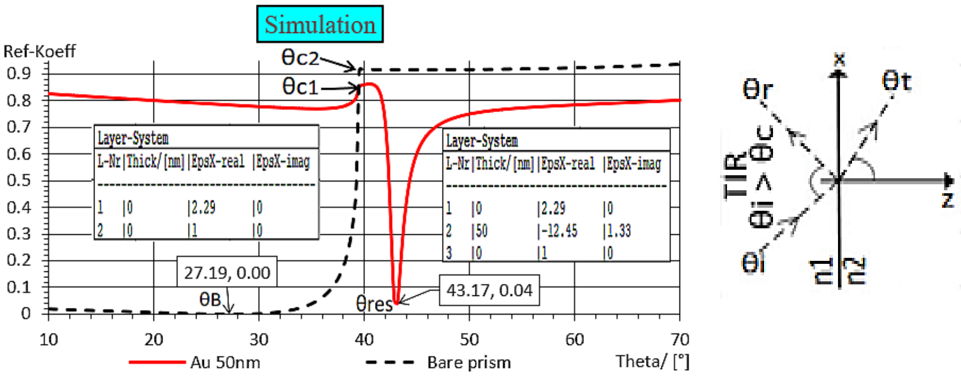

Figure 6. P-polarized on Brewster's and resonance angle

(a)

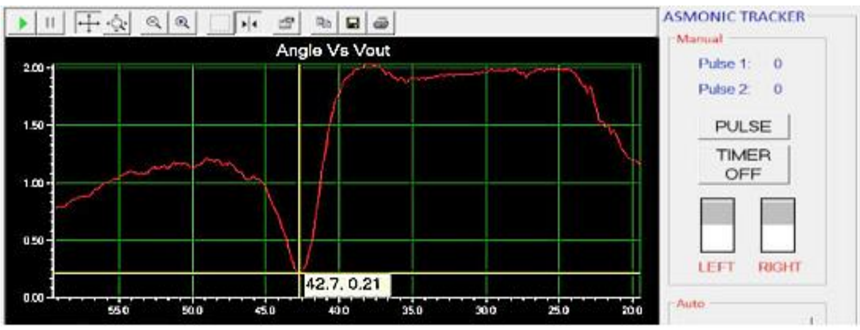

(b)

Figure 7. Measured reflectivity traces from (a) bare prism and (b) coated prism with 50 nm Au layer

Referring to the Figure 8, images of the reflected beams from coated (50 nm gold layer) and non-coated prism were captured by a compact complementary metal-oxide-semiconductor (CMOS) camera at 43°. Lower/higher RGB values in Table 2 indicate the presence/absence of the plasmonic energy, as shown in Figure 8(a) and Figure 8(b), respectively. a signal processing technique via least fitting polynomial successfully smoothing noisy data in Figure 9. A high-frequency fluctuation was observed in Figure 9(a) and smoothed out until ten filtering stages in Figure 9(b) with the Savitzky-Golay (SG) algorithm.

Table 2. RGB values of the reflected beam

Prism	Angle	Mean values			SD values		
		R	G	B	R	G	B
Au Coated (50 nm)	43	40.82	8.83	20.57	41.35	3.75	4.68
Non-coated	43	139.66	38.84	56.17	93.65	83.13	80.71

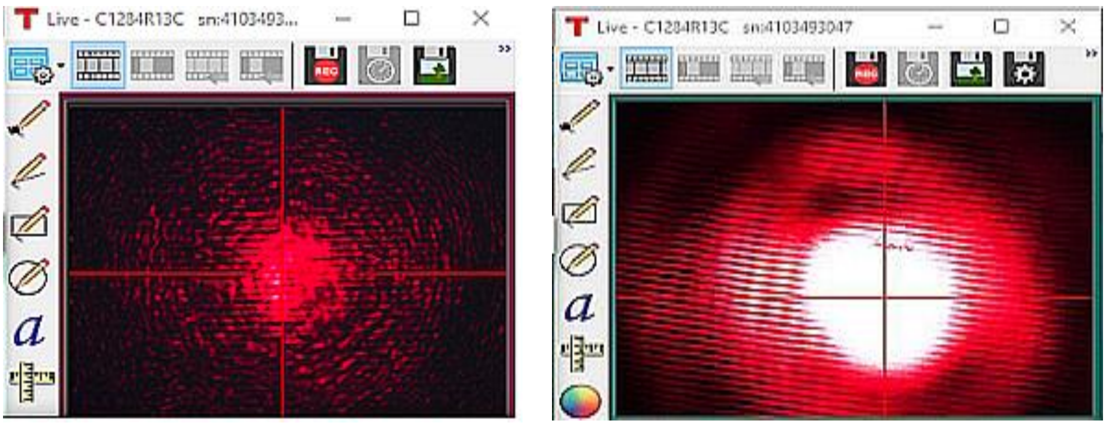

(a) (b)

Figure 8. Images from (a) coated prism with 50 nm Au layer and (b) non-coated prism

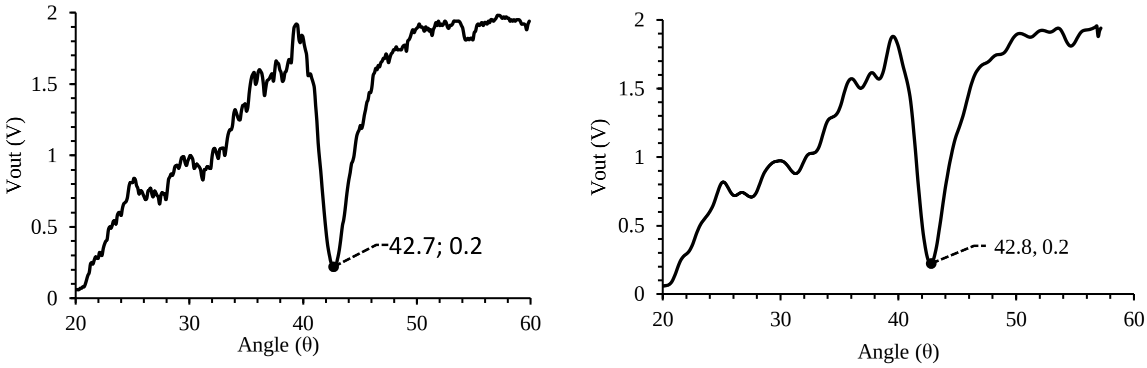

(a) (b)

Figure 9. Reflective traces (a) before filter and (b) after SG filtering

4. CONCLUSION

3D printing modular optomechatronics system components reduced development costs. Modular printing and assembly were made possible. Generating plasmonic energy under P-polarization satisfies the boundary condition of the metal-dielectric interfaces. The reflectivity trace indicates a resonance angle at 42.7° (θres), while critical angles for coated (θ_{C1}) and non-coated (θ_{C2}) prism were observed at 39°. The absence of a thin gold layer at 50 nm could not generate the plasmonic energy. Vice versa, the coated thin layer at 50 nm on the prism indicates maximum attenuation immediately beyond the critical angle. A low-cost 3D-printed optomechatronics device was shown to be a reliable, accurate, and efficient plasmonic-based biosensor.

ACKNOWLEDGEMENTS

This study was funded by the Malaysia Ministry of Higher Education through the Fundamental Research Grant Scheme (FRGS) FRGS/1/2020STK0/UNIKL/02/5 and supported by Nutrition, Metabolic and Cardiovascular Research Centre (NMCRC), Institute for Medical Research, Ministry of Health Malaysia.

REFERENCES

[1] V. R. Samuel and K. J. Rao, “A review on label free biosensors,” *Biosensors and Bioelectronics: X*, vol. 11, Art. no. 100216, Sep. 2022, doi: 10.1016/j.biosx.2022.100216.

[2] G. Nava, G. Zanchetta, F. Giavazzi, and M. Buscaglia, “Label-free optical biosensors in the pandemic era,” *Nanophotonics*, vol. 11, no. 18, pp. 4159–4181, Aug. 2022, doi: 10.1515/nanoph-2022-0354.

[3] T. Kadja, “Intelligent real-time polymerase chain reaction system with integrated nucleic acid extraction for point-of-care medical diagnostics,” PhD Thesis, University of Dayton, University of Dayton, 2023. Accessed: Nov. 27, 2023. [Online]. Available: http://rave.ohiolink.edu/etdc/view?acc_num=dayton1689788275578789

[4] O. T. Kwon, G. Kim, H. Bae, J. Ryu, S. Woo, and B. K. Cho, “Development of a mercury bromide birefringence measurement system based on Brewster’s angle,” *Sensors*, vol. 23, no. 9, Art. no. 4208, Apr. 2023, doi: 10.3390/s23094208.

[5] T. Li, G. Liu, H. Kong, G. Yang, G. Wei, and X. Zhou, “Recent advances in photonic crystal-based sensors,” *Coordination Chemistry Reviews*, vol. 475, p. 214909, Jan. 2023, doi: 10.1016/j.ccr.2022.214909.

[6] G. Qiu, Z. Gai, Y. Tao, J. Schmitt, G. A. Kullak-Ublick, and J. Wang, “Dual-functional plasmonic photothermal biosensors for highly accurate severe acute respiratory syndrome coronavirus 2 detection,” *ACS Nano*, vol. 14, no. 5, pp. 5268–5277, Apr. 2020, doi: 10.1021/acsnano.0c02439.

[7] Biosensors Market, “Biosensors market size, share, trends and revenue forecast [Latest],” *Biosensors Market*. https://www.marketsandmarkets.com/Market-Reports/biosensors-market-798.html (accessed Sep. 21, 2023).

[8] J. Slabý and J. Homola, “Performance of label-free optical biosensors: What is figure of merit (not) telling us?,” *Biosensors and Bioelectronics*, vol. 212, p. 114426, Sep. 2022, doi: 10.1016/j.bios.2022.114426.

[9] Y. S. Chen, C. H. Huang, P. C. Pai, J. Seo, and K. F. Lei, “A review on microfluidics-based impedance biosensors,” *Biosensors*, vol. 13, no. 1, p. 83, Jan. 2023, doi: 10.3390/bios13010083.

[10] A. K. Singh, S. Mittal, M. Das, A. Saharia, and M. Tiwari, “Optical biosensors: a decade in review,” *Alexandria Engineering Journal*, vol. 67, pp. 673–691, Mar. 2023, doi: 10.1016/j.aej.2022.12.040.

[11] M. B. Kulkarni, N. H. Ayachit, and T. M. Aminabhavi, “Recent advances in microfluidics-based electrochemical sensors for foodborne pathogen detection,” *Biosensors*, vol. 13, no. 2, p. 246, Feb. 2023, doi: 10.3390/bios13020246.

[12] J. Tang, G. Qiu, and J. Wang, “Recent development of optofluidics for imaging and sensing applications,” *Chemosensors*, vol. 10, no. 1, p. 15, Jan. 2022, doi: 10.3390/chemosensors10010015.

[13] Ravina, A. Dalal, H. Mohan, M. Prasad, and C. S. Pundir, “Detection methods for influenza A H1N1 virus with special reference to biosensors: A review,” *Bioscience Reports*, vol. 40, no. 2, Feb. 2020, doi: 10.1042/BSR20193852.

[14] U. Jain, N. Chauhan, and K. Saxena, “Fundamentals of sensors and biosensors: An overview,” in *Multifaceted Bio-sensing Technology*, Elsevier, 2023, pp. 31–44. doi: 10.1016/b978-0-323-90807-8.00005-1.

[15] A. Cossettini, J. Vidic, M. Maifreni, M. Marino, D. Pinamonti, and M. Manzano, “Rapid detection of Listeria monocytogenes, Salmonella, Campylobacter spp., and Escherichia coli in food using biosensors,” *Food Control*, vol. 137, p. 108962, Jul. 2022, doi: 10.1016/j.foodcont.2022.108962.

[16] T. Anjum, N. Hussain, M. Bilal, and H. M. N. Iqbal, “Enzymatic biosensors,” in *Biocatalyst Immobilization*, Elsevier, 2023, pp. 341–363. doi: 10.1016/b978-0-323-91317-1.00006-2.

[17] G. K. Ali and K. M. Omer, “Molecular imprinted polymer combined with aptamer (MIP-aptamer) as a hybrid dual recognition element for bio(chemical) sensing applications. Review,” *Talanta*, vol. 236, Art. no. 122878, Jan. 2022, doi: 10.1016/j.talanta.2021.122878.

[18] M. A. Morales and J. M. Halpern, “Guide to selecting a biorecognition element for biosensors,” *Bioconjugate Chemistry*, vol. 29, no. 10, pp. 3231–3239, Sep. 2018, doi: 10.1021/acs.bioconjchem.8b00592.

[19] T. Fatima, S. Bansal, S. Husain, and M. Khanuja, “Biosensors,” in *Electrochemical Sensors: From Working Electrodes to Functionalization and Miniaturized Devices*, Elsevier, 2022, pp. 1–30. doi: 10.1016/B978-0-12-823148-7.00001-5.

[20] W. Hussain, M. W. Ullah, U. Farooq, A. Aziz, and S. Wang, “Bacteriophage-based advanced bacterial detection: Concept, mechanisms, and applications,” *Biosensors and Bioelectronics*, vol. 177, Art. no. 112973, Apr. 2021, doi: 10.1016/j.bios.2021.112973.

[21] M. R. Abdullah, N. H. Harun, and R. A. A. Raof, “Microstepping synchronization via hybridization of Mamdani’s Fuzzy Logic for the plasmonic tracker,” *Journal of Physics: Conference Series*, vol. 1997, no. 1, p. 12033, Aug. 2021, doi: 10.1088/1742-6596/1997/1/012033.

[22] J. X. J. Zhang, “Plasmonic MEMS in biosensing and imaging,” in *Synthesis Lectures on Materials and Optics*, Springer International Publishing, 2023, pp. 107–181. doi: 10.1007/978-3-031-23137-7_5.

[23] M. R. Abdullah and N. H. Harun, “A microfluidic channel and light refraction simulation for micro-organism identification,” in *2017 International Conference on Engineering Technology and Technopreneurship, ICE2T 2017*, Sep. 2017, vol. 2017-Janua, pp. 1–5. doi: 10.1109/ICE2T.2017.8215989.

[24] C. Zhan, J. Yi, S. Hu, X. G. Zhang, D. Y. Wu, and Z. Q. Tian, “Plasmon-mediated chemical reactions,” *Nature Reviews Methods Primers*, vol. 3, no. 1, Feb. 2023, doi: 10.1038/s43586-023-00195-1.

[25] M. R. Abdullah and N. H. Harun, “Preliminary study in microfluidic channel and gold nanoparticles with finite element simulation on biosensor development,” in *AIP Conference Proceedings*, 2019, vol. 2129. doi: 10.1063/1.5118130.

[26] A. Dante *et al.*, “Development of an Escherichia coli optical biosensor with computational validation,” *Journal of Physics: Conference Series*, vol. 2407, no. 1, p. 12029, Dec. 2022, doi: 10.1088/1742-6596/2407/1/012029.

[27] V. Fallahi, Z. Kordrostami, and M. Hosseini, “A solution for detection of ethanol and methanol with overlapping refractive indexes based on photonic crystal ring resonator optical sensors,” *IEEE Sensors Journal*, vol. 23, no. 7, pp. 6791–6798, Apr. 2023, doi: 10.1109/JSEN.2023.3249626.

BIOGRAPHIES OF AUTHORS

Muhammad Rosli Abdullah received a BSc in medical electronics from the University of Hertfordshire, United Kingdom, and an MSc in electrical, electronics, and systems from the National University of Malaysia. Currently, he is a PhD student at the Universiti of Kuala Lumpur. His research interests include biosensor technology, plasmonics, photonics, medical instrumentation, embedded systems, software interfacing, machine learning, and electronics systems. He can be contacted at rosli@unikl.edu.my.

Noor Hasmiza Harun received a B.Eng degree in medical electronics from the University of Technology Malaysia and an MSc. and PhD. in instrumentation engineering from the University of Putra Malaysia. Her research interests include electromagnetic sensors, biomedical instrumentation, biomedical signal processing, and rehabilitation engineering. She can be contacted at noorhasmiza@unikl.edu.my.

Siti Noorjannah Ibrahim received a B.Eng degree in electronics engineering from the University of Technology Malaysia, an MSc in microelectronic systems and telecommunication from Liverpool University, United Kingdom and a PhD in Nanostructure Science and Technology from University of Canterbury, New Zealand. Her research interests are on the fundamental studies and applications related to micro-nano fluidic channels, the interface of biological cells, biomedical instrumentations, and wireless communications technologies (internet of things). She can be contacted at email: noorjannah@iium.edu.my.

Azimah Abdul Wahab is a senior lecturer at the Clinical and Biomedical Laboratory Science Section, Universiti Kuala Lumpur-Institute of Medical Science Technology. She attained her PhD in virology at the University of Surrey, UK, and her main research interest is microbiology (Virology). She can be contacted at azimahaw@unikl.edu.my.

Mohd Azerulazree Jamilan works at the Cardiovascular, Diabetes, Endocrine and Nutrition Research Centre, Institute for Medical Research National Institutes of Health, Ministry of Health Malaysia, Shah Alam, Malaysia. His primary interest is in nutrition electrochemistry and analytical chemistry. He can be contacted at azerulazree@moh.gov.my.